Critical Power for Lower Hybrid Current Drive

Altair S. de Assis[1], Paulo H. Sakanaka[2], Carlos A. de Azevedo[3], and José Busnardo Neto[2]

[1] *Universidade Federal Fluminense, GMA 24020-000, Niterói, RJ, Brazil*

[2] *Instituto de Física 'Gleb Wataghin', Universidade Estadual de Campinas, UNICAMP, 13083-970, Campinas, São Paulo, Brazil*

[3] *Instituto de Física, Universidade do Estado do Rio de Janeiro 20550-013, Rio de Janeiro, RJ, Brazil*

Received April 29, 1996

We have solved numerically the quasilinear Fokker-Planck equation which models the critical power for lower hybrid wave current drive. An exact value for the critical power necessary for current saturation, for tokamak current drive experiments, has been obtained. The nonlinear treatment presented here leads to a final profile for the parallel distribution function which is a plateau only in a part of the resonance region. This form of the distribution function is intermediate between two well known results: a plateau through out the resonance region for the linear strong-source regime, $D_{wave} \gg D_{coll}$ and no plateau at all in the resonance region for the linear weak-source regime, $D_{wave} \ll D_{coll}$ [1]. The strength of the external power source and the value of the dc electric field are treated as given parameters in the integration scheme.

I. Introduction

The principle of the lower hybrid current drive (LHCD) was demonstrated in the Japanese tokamak JFT-2[2], in this experiment ohmic heating was present. The start up of a plasma without the aid of inductive ohmic current was later proved possible by Kubo et al[3]. The theoretical basis for this scheme of current generation was proposed by Fisch[4] and since then a vast amount of research work both theoretical and experimental has been dedicate to this subject. See for instance references [1] - [12], and the references cited therein.

There are, in general, two approaches to study the, radiofrequency (rf) current drive. In the first model, the Fokker-Planck equation is solved for fixed radio frequency diffusion coefficient, in this case one has to solve a linear differential equation with respect to the distribution function f, we call this model here non self-consistent[1,7,8]. The second approach, considers the injected radio frequency power density fixed with given spectral shape due to the antenna. In this approach, the diffusion coefficient depends on the derivative of the distribution function f, the differential equation that models f then becomes nonlinear with respect to f, we label this model as self-consistent with respect to the external power[10].

Even though the non self-consistent model reproduce all the important dependencies of the LHCD process such as those on density, temperature, applied power, and applied rf spectrum, both in a qualitative and in a quantitative way, it cannot predict when the generated current will stop growing with respect to the applied rf power and when it will saturate at some maximum current level. Consequently, this model cannot predict, in real experiments, since the critical power is not known, the amount of external power that is lost due to current saturation. Once the plateau has been reached, the extra amount of power injected is lost as far as the current generation problem is concerned. Knowing the critical power level for current saturation, it is possible to save power during the LHCD shot. Of course, during the experimental phase of the current drive, power can be lost without being much criticized, since the main goal is to prove the viability of the process. However, in the final phase of fusion research it will be compulsory to use the correct amount of power. More power injected than the necessary will reduce the real efficiency of the reactor. Note that the physical efficiency does not account for this lost since it is defined using the dissipated power and not the injected one. Note that when 100% of the external power is absorbed by the plasma the dissipated power is equal to the injected one ($P_d = \int 1/2mv^2 \partial f/\partial t dv = P_{rf}$), however this is not the case in real LHCD tokamak experiments[1,5] and, in this way, the physical efficiency is much lager than the real one. So, we can state that the non self-consistent model is related to the absorbed power and our self-consistent with the external injected one. It is necessary to say that a self-consistent LHCD theory in the sense of $k_\parallel$ spectrum has been already developed by Bonoli and Englade[8]. However, the diffusion coefficient, in this model, is not a functional of f and therefore with this model one cannot access the critical power information. So, our self-consistency has a different meaning of the one reported by Bonoli and Englade[8].

In order to access the critical power level, we use a quasilinear Fokker- Planck model considering the dependence of the velocity space diffusion coefficient on the injected power level[10-12]. We recall that our self-consistent linear model usually considers two regimes[11,14]: the **weak-source** regime, where the nonresonant collisional damping is much smaller than the collisionless Cherenkov damping, and the **strong-source** regime in which the reverse is true. In the first case, the rf power level is low and it is not sufficient to form a plateau in the resonant region of the distribution function and therefore the derivative $\partial f/\partial v_\parallel$ plays an important role. In the strong-source regime a plateau is formed in the resonant region of velocity space, therefore $\partial f/\partial v_\parallel \simeq 0$. In both cases, the system of equations is linear which is easily treated. Examples are abundant in the literature.

See, for instance, Ref. [10] and references cited therein. The intermediate case is nonlinear and has not been yet treated in the literature. This paper is organized as follows. In section II, we consider the basic equations. In section III, we present the numerical results valid for tokamaks such as the JT-60 where LHCD was first applied to a large tokamak. In the section IV we obtain the critical power for current saturation. In section V, we present our conclusions. The cgs system of units is used throughout this paper.

II. Fokker-Planck quasilinear equations

The one dimensional Fokker-Planck quasilinear system of equation suitable to study, in a self-consistent way, current drive and runaway electron flux, induced by lower hybrid waves, is given by [9, 10]

$$\frac{\partial F}{\partial t} = \frac{\partial}{\partial v_\parallel}\left[D\{F,t\}\frac{\partial F}{\partial v_\parallel}\right] + \frac{\nu_0}{v_\parallel^3}\left[v_\parallel F + \frac{\partial F}{\partial v_\parallel}\right] - E\frac{\partial E}{\partial v_\parallel} \tag{1}$$

with

$$D\{F,t\} = \frac{1}{2\pi v_\parallel^3}\int_0^{\pi/2} d(\cos\theta)\cos\theta U_{k=1/v_\parallel} \tag{2}$$

and

$$\frac{\partial U_{\vec{k}}}{\partial t} = 2\left(I_m\omega_{\vec{k}} - \frac{\nu_{col}}{2}\right)U_{\vec{k}} + S_{\vec{k}} \tag{3}$$

with

$$I_m\omega_{\vec{k}} = \frac{\pi}{2}\cos\theta\frac{\partial F}{\partial v_\parallel}|_{v_\parallel=1/k} \tag{4}$$

The stable stationary solution of Equation (1) is given by considering $\partial/\partial t \equiv 0$. Thus, from the Equations (1)-(4) one finds the nonlinear eigenvalue problem for A and F, that is:

$$\left(1+\tilde{D}\{F\}v_\parallel^3\right)\frac{dF}{dv_\parallel} + (v_\parallel - \tilde{E}v_\parallel^3)F - \tilde{A}v_\parallel^3 = 0 \tag{5}$$

where $\tilde{E} = E/\nu_0$; $A = A/\nu_0$; $D\{F\} = D\{F\}/\nu_0$.

Equation (5) is also suitable to study the critical power for the current drive and enhancement of runaway production processes. Here, $F(v_\parallel)$ is the quasilinear averaged parallel electron distribution function, which follows a slow time scale evolution due to the lower hybrid waves, binary collisions, and the dc electric field. The term $U_{\vec{k}}$ is the spectral energy density of the lower hybrid wave, $Im(\omega_{\vec{k}}^{LH})$ is the collisionless Cherenkov damping coefficient, ν_{coll} is the collisional nonresonant damping and, finally, $S_{\vec{k}} = (\nabla\cdot\vec{P})_{\vec{k}}$ is the term that models the external radio frequency power source[10,11,16], where $\vec{P}$ is the Poynting's vector.

The normalization is given by (**un $\equiv$ unnormalized quantities**):

$$v_{\parallel}^{un} = v_{\parallel} v_{the} \qquad (6)$$
$$k^{un} = k\lambda_{De} \qquad (7)$$
$$t^{un} = t\omega{-}1_{pe} \qquad (8)$$
$$f^{un}(v_{\parallel}, v_{\perp}) = f(v_{\parallel} v_{\perp} N_e v_{the}^{-3} \qquad (9)$$
$$E^{un} = E(4\pi N_e T_e)^{1/2} \qquad (10)$$
$$U_{\vec{k}}^{un} = U_{\vec{k}}(4\pi N_e T_e \lambda_{De}^{-3} \qquad (11)$$

Where v_{the}, λ_{pe}, N_e, and T_e are the electron thermal velocity, the electron Debye length, the electron plasma frequency, the electron plasma density, and finally the electron temperature, respectively.

We take the parallel distribution function $F(v_{\parallel})$ as defined by the relation

$$f(v_{\perp}, v_{\parallel}) F_m(v_{\perp}) F(v_{\parallel})$$

where $F_M(v_{\perp})$ is the fixed Maxwellian distribution function and $F(v_{\parallel})$ is the part to be determined by solving the nonlinear Fokker-Planck quasilinear system of equations. This approximation is a rather reasonable one to study the posed problem since the main dynamics in the Cherenkov interaction occurs in the parallel direction[1,15,17,18]. It should be mentioned that Bonoli and Englade[8] have discussed the effect of taking $T_{perp} \neq T_{parallel}$ on the diffusion coefficient for the linear regime. However, for the nonlinear case this is still an open problem and it will be addressed in future work since it is out of the scope of the present paper.

The external source $S_{\vec{k}}$ is given by [9]

$$S_{\vec{k}} = \begin{cases} S\delta(\cos\theta - \cos\theta_0)[H(k-k_1) - H(k-k_2)] & \text{for } k_1 \leq k \leq k_2 \\ 0 & \text{elsewhere} \end{cases} \qquad (12)$$

where k is the parallel wave number which is related to $v_{\parallel}$ through the resonance condition and the dispersion relation for lower hybrid waves. From Equations (2), (3), (4) and (12) the diffusion coefficient $D\{F(v_{\parallel})\}$ can be written as follows[10]

$$D\{F(v_{\parallel})\} = \frac{S\cos\theta_0}{8\pi} \frac{[H(k-k_2) - H(k-k_1)]}{v_{\parallel}^3 \left[\nu_{coll} - \pi\cos\theta k^{-2} \frac{\partial F}{\partial v_{\parallel}}|_{v_{\parallel}=1/k}\right]} . \qquad (13)$$

From Equation (13) we see that the diffusion coefficient D has a functional dependency on $F(v_{\parallel})$ and therefore, substitution of Equation (13) into Equation(5) leads to a nonlinear differential equation for $F(v_{\parallel})$. Note that $\frac{\partial F}{\partial v_{\parallel}} < 0$, always, since we are dealing with dissipation and not with instability, therefore the denominator of $D\{F(v_{\parallel})\}$ never vanishes. The relation between ν_{coll} and $\cos\theta_0$ $k^{-2}\frac{\partial F}{\partial v_{\parallel}}$ determines the three possible regimes (linear- linear, nonlinear, and linear-plateau). Note that here ν_{coll} is fixed but $\frac{\partial F}{\partial v_{\parallel}}$ varies with the rf power.

The dc electric field term is given elsewhere[19,21,22], and A is the necessary particle source term since a stationary distribution function involving a loss of particles at plus infinity implies an equivalent source at $v_{\parallel} = 0$ [20, 21]. If no electric field is present (no runaway electron production), $A = 0$. More details about the terms that appear in the nonlinear system can be found elsewhere, for instance, Refs. [9, 10, 12]. In this paper, we solve (5) numerically and plot $F(v_{\parallel})$ and A as a function of the external lower hybrid source strength and the DC electric field (A=A(S,E)), using the normalization given by the Equations (6)-(11).

III. Critical Power for rf Current Drive

It is in order now to define what we call here critical power for rf current drive. In convenient units the needed power to sustain a rf current I defined as

$$I = 6.7 \times 10^4 n[10^{19} m^{-3}] T_e^{1/2} a^2 [m^2] j$$

where

$$j = \int_{-\infty}^{+\infty} F(v_{\parallel}) v_{\parallel} dv_{\parallel} ,$$

is given by:

$$P(MW) = 2.9 \times 10^8 R[m] a^2 [m^2] n^{3/2} [10^{19} m^{-3}] T_e [keV] S \tag{14}$$

where S is defined in Equation (12). We can then write the critical power as below. Note that the critical power is the minimum power needed for current saturation and can be known once S_c in known.

$$P_c(MW) = 2.9 \times 10^8 V_{ef} [m^3] T_e [keV] N_e^{3/2} S_c \tag{15}$$

With $V_{ef} \leq V_{real} = Ra^2$ being the volume where the rf wave power is deposited in the tokamak, 'R' is the tokamak major radius, 'a' is the minor radius, and S_c is the minimum normalized spectral amplitude for which the current saturates. This value is given from the numerical or analytical solution of Equation (5). Thus, using the above formula and considering the JT-60U data during the LHCD event reported by Ushigusa et al.[6], we can see that the situation $P_{rf} < P_c$ occurs. It means that the LHCD regime for the JT-60U, in this event, is linear but, however, not very far from the saturation level. The critical regime can be reached in this case for $N_e \approx 0.5 \times 10^{19} m^{-3}$; $T_e \approx 2keV$; $P_{rf} \approx 2MW$; $V_{ef} \approx 1\% V_{real}$. The real power deposition volume can be obtained from the toroidal ray tracing theory[8][24].

For ITER tokamak conception[23] we have also $P_{rf} < P_c$. Note that our numerical calculation shows the saturation level at $S = 10^{-7}$ and for ITER it means $P_c \approx 10^3$MW. Thus, to match the $P_{rf} \approx 50$MW reported in reference [23] for ITER LHCD, we have to have $S \approx 10^{-9}$ which corresponds to a linear regime according to our numerical results.

IV. Numerical results and discussion

Here, we present numerical results valid to model the data for several different tokamaks, for example the Japanese tokamak JT-60U. The normalized power S varies from 10^{-9} to $10^{7/3} \times 10^{-9}$ and covers the JT-60U LHCD regime[6,13]. We solved the nonlinear eigenvalue Equation (5) using a fourth-order Runge-Kutta method. From now on, we will write v instead of $v_{\|}$.

The results of the numerical evaluation of Equation (5) for F(v) are shown in Figs. 1-4 as a function of the normalized external power strength S and the electric field E. In Fig. 1, we show the plot of the distribution function F versus the velocity v for different values of the external power strength and electric field intensity E = 0. The resonance width considered was a typical value for tokamaks $\Delta v = 2v_{the}$ with $v_1 = 4v_{the}$ and $v_2 = 6v_{the}$. Here, v_{the} is defined as $v_{the} = \sqrt{(T_e/m_e)}$. The angle θ_0 was fixed as 45° [9, 10, 11].

It is seen from the figure that the formation of the plateau starts at the lower limit of the resonance region, precisely at the beginning of the nonlinear regime governed by the nonlinear differential, Equation (5). Then, we see an intermediate plateau solution is which is not maintained to the upper limit of the resonance region. This intermediate plateau solution, is only possible in the nonlinear regime reported here.

In Fig. 2, we have again the distribution function F versus the velocity v but with a nonzero electric field and we see that the intermediate plateau occurs at a different level and also that it is formed slightly before the E = 0 case for the same power level.

In Fig. 3, we show once more the distribution function F versus the ve- locity v but with the electric field slightly higher than that of Fig. 2 and again we see the intermediate plateau formation at a different level and also it is formed slightly before than the E = 0 and E = 0.01 cases, for the same power level.

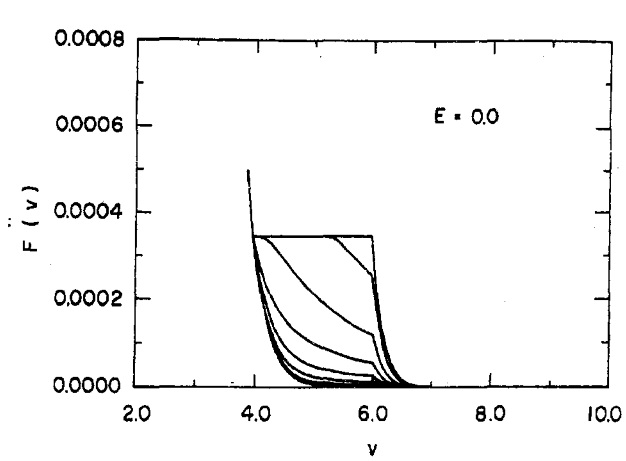

Figure 1. Normalized electron distribution function F versus normalized parallel velocity v for $E = 0$ and: $S = 10^{-9}, 10^{1/3}10^{-9}, 10^{2/3}10^{-9}\ 10^{-8}\ 10^{4/3}10^{-9}\ 10^{5/3}10^{-9}\ 10^{-7}\ 10^{7/3}10^{-9}$.

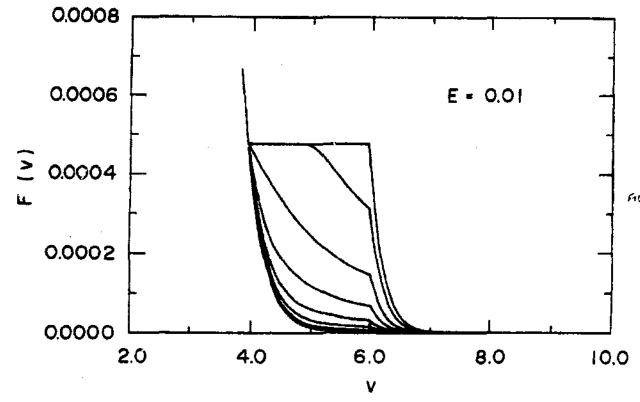

Figure 2. Normalized electron distribution fimction F versus normalized parallel velocity v for $E = 0.01$ and: $S = 10^{-9}, 10^{1/3}10^{-9}, 10^{2/3}10^{-9}\ 10^{-8}\ 10^{4/3}10^{-9}\ 10^{5/3}10^{-9}\ 10^{-7}\ 10^{7/3}10^{-9}$.

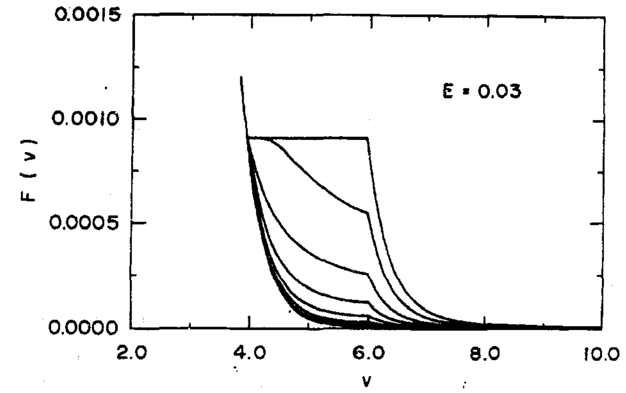

Figure 3. Normalized electron distribution function F versus normalized parallel velocity v for $E = 0.01$ and: $S = 10^{-9}, 10^{1/3}10^{-9}, 10^{2/3}10^{-9}\ 10^{-8}\ 10^{4/3}10^{-9}\ 10^{5/3}10^{-9}\ 10^{-7}\ 10^{7/3}10^{-9}$.

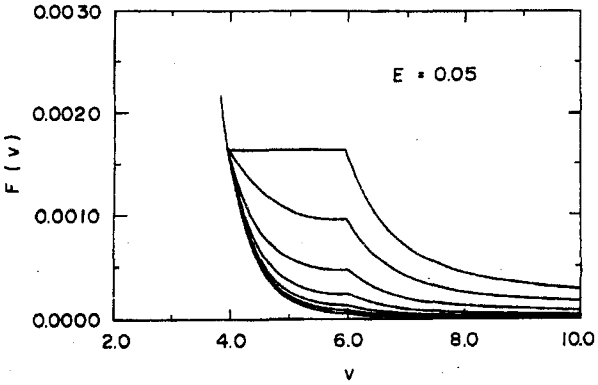

Figure 4. Normalized electron distribution function F versus normalized parallel velocity v for $E = 0.05$ and: $S = 10^{-9}, 10^{1/3}10^{-9}, 10^{2/3}10^{-9}\ 10^{-8}\ 10^{4/3}10^{-9}\ 10^{5/3}10^{-9}\ 10^{-7}\ 10^{7/3}10^{-9}$.

In Fig. 4, we show the same results as in the last three cases using the same parameters but with a stronger applied electric field, E = 0.05. It is seen in this case that there is no plateau formation at all. The reason is that the Landau damping coefficient affected by the applied electric field, We see the runaway tail formation in the distribution function.

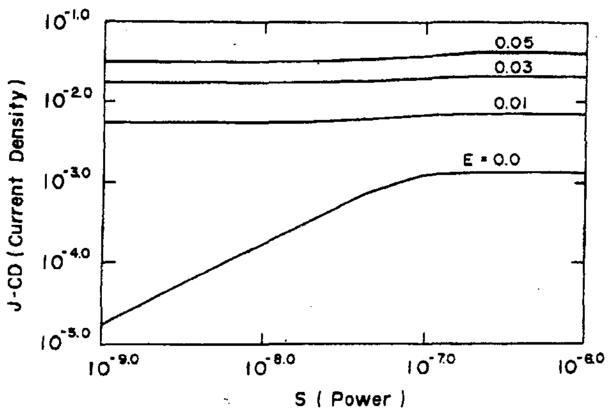

Figure 5. Normalized parallel rf current density J_{CD} versus normalized rf wave power S, for $E = 0.00, 0.01, 0.03, 0.05$.

In Fig. 5, we present a plot of the current driven versus the external power strength for three values of the electric field. We see from the plot that the saturation level is shown explicitly without any extrapolation and the critical power is shown to be $S = 10^{-7}$. Note that the power for the beginning of the plateau formation is the same power for the beginning of current saturation; that is, the critical power for rf current drive.

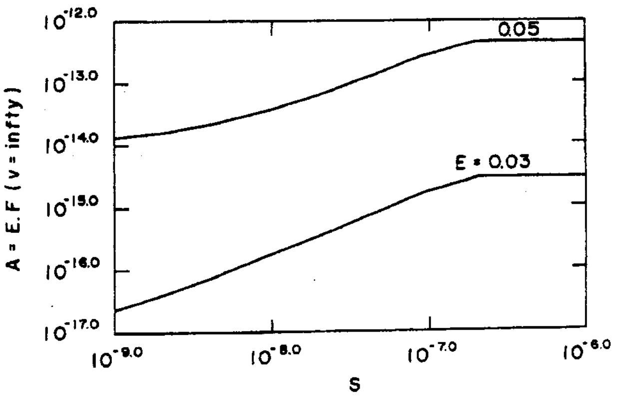

Figure 6. Normalized runaway flux A versus normalized rf wave power S, for $E = 0.03$, 0.05.

In Fig. 6, we consider the runaway production rate A, treated here as a nonlinear eigenvalue of Equation (5). Saturation can be seen from the plot. The flux enhancement and the saturation level occurs around $S = 10^{-7}$. The plot also shows that the enhancement of the runaway flux induced by the presence of the lower hybrid wave is larger the weaker the applied dc electric field. The runaway flux in the case of E = 0.01 is not presented since this flux is very small. Only a direct acceleration by a DC electric field can generate runaway flux. Radio frequency waves alone cannot do it, therefore the flux vanishes for E = 0. Radio frequency waves do not cause runaway production since they interact with electrons only in the resonance region.

Finally, we can assure that the intermediate plateau shown in the plots is caused by the nonlinearity, since the 1D result, for the electron distribution function. presented in the basic paper Fisch[1,4], does not account for the second solution of $\frac{\partial F}{\partial v_{\parallel}}$. Only the complete plateau is a possible solution in the Fisch's[4], model. and. of course, in the all other non self-consistent models[1].

V. Conclusions

In the present paper we have discussed the critical power problem for rf current drive, we call critical power the minimum power needed for rf current saturation. It can only be correctly accessed using the nonlinear approach presented here since we can plot current versus injected power. In the widely used non self-consistent approach (D imposed) the efficiency is known only via the dissipated power and therefore the information about the critical power remains unknown. Note that $S_{\bar{k}}$ was treated here with a certain degree of freedom. This term might be interpreted in our model as the source of the wave spectrum in a kind of "back-body" model in which the plasma cavity is permeated by radio frequency waves. So, $S_{\bar{k}}$ can be chosen by the grill theory and modified in a parametric fashion in order to evaluate its effects on the rf current[10]. The knowledge of the critical power prevents the use of radio frequency power after the saturation level has been reached, and this is important from the practical point of view since high power microwave sources are expensive and the knowledge of the minimum power needed for current saturation is desirable.

It is very clear from our plots that the plateau formation starts from the lower resonant velocities and proceeds to the higher ones. This allows the possibility of designing the antenna so that power can be saved if one moves the power after the intermediate plateau is formed to the high velocity side of the resonance region. This plateau formation feature is due to the structure of the nonlinear equation. However, further investigation of this kind of nonlinear equation is necessary. The formation of an intermediate plateau is only possible due to the nonlinearity. It is very clear from our plots that the electric field affects the intermediate plateau formation considerably since it affects both the nonlinearity of the differential equation and the Landau damping process itself. For the same level of external applied power the plateau is different for different fields.

A complete view of the posed problem in this paper requires further investigation which is left for a future work. For example, a natural extension of this investigation would be to introduce more realistic absorbed power density[8,24], inhomogeneities[24], two dimensions in velocity space[8] and the anomalous Doppler interaction[9].

Acknowledgements

This work was supported by the Brazilian agencies CNPq - Conselho Nacional de Desenvolvimento Tecnológico e Científico, FAPESP - Fundação de Amparo à Pesquisa do Estado de São Paulo, FAPERJ - Fundação de Amparo Pesquisa do Estado do Rio de Janeiro and FINEP - Financiadora de Estudos e Projetos.

References

1. N. J. Fisch, Rev. Mod. Phys., **59**, 175 (1987).
2. T. Yamamoto, et al., Phys. Rev. Lett. 716 (1980).
3. H. Kubo, et al., Phys. Rev. Lett. **50**, 1994 (1983).
4. N. J. Fisch, Phys. Rev. Lett. **41**, 873 (1978).
5. T. Watari, *Review of Japanese Results on Heating and Current Drive,* Plasma Phys. Contr. Fusion, **35**, A A181-A198 (1993).
6. K. Ushigusa, T. Kondoh, O. Naito, Y. Ikeda, S. Ide, M. Seki, S. W. Wolfe, M. Sato, Y. Kamada, K. Itami and T. Imai, Nuclear Fusion, **32**, 11 (1992). S. Ide, T. Imai, K. Ushigusa, O. Naito, Y. Ikeda, M. Nemoto and M. Sato, Nuclear Fusion, **32**, 2 (1992).
7. C. F. F. Karney, Computer Phys. Rep. **4**, 183 (1986).
8. P. T. Bonoli and R. C. Englade, Phys. Fluids, **29**, 9 (1986).
9. L. M. Muschietti, J. Vaclavik and K. Appert, Plasma Phys., **24**, 8 (1982).
10. S. Succi, *Quasilinear Modelling of Lower Hybrid Current Drive and Related Problems,* Ph D thesis, EPFL-CRPP, Lausanne, Suisse, (1987).
11. S. Succi, K. Appert, J. Muschietti and J. M. Werringer, Phys. Lett., **106A**, 137 (1984).
12. J. Vaclavik, K. Appert, A. H. Kritz and L. Muschietti, Plasma Phys., **25**, 1295 (1983).
13. Y. Takase, M. Honda, Y. Ikeda, T. Imai, K. Sakamoto, S. Tsuji, K. Uehara and K. Ushigusa, Nuclear Fusion, **28**, 6 (1988).
11. Y. Takase, et al., Nuclear Fusion, **28**, 1112 (1988).
15. A. S. de Assis and J. Busnardo-Neto, Phys. Fl., **31**, 943 (1988).
16. C. Bruder, J. Vlaclavik and K. Appert, *Nonlinear Interaction of Lower Hybrid Waves, in Joint Varena-Lausanne International Workshop on "Theory of Fusion Plasmas",* Varena, Italy, (1991).
17. A. Hasegawa and K. Mima, J. Geophys. Res., **83**, 1117 (1978).
18. A. S. de Assis and J. Busnardo-Neto, Il Nuovo Cimento, **104B**, 263 (1989).
19. R. M. Kulsrud, Y.-Ch. Sun and H. A. Fallon, Phys. Rev. Lett., **31**, 690 (1973).
20. C. S. Liu, Z. G. An, D. A. Boyd, Y. C. Lee, L. Muschietti, K. Appert and J. Vaclavik, Comments Plasma Phys. Contr. Fusion, **7**, 2 (1982).
21. V. V. Parail and O. P. Pogutse, Nucl. Fusion, **18**, 303 (1978).
22. Z. G. An, C. S. Liu, Y. C. Lee and D. A. Boyd, Phys. Fluids, **25**, 997 (1982).
23. F. Engelmann et al., (European Coordinating Committee on Lower Hybrid Waves (CCLH)), *Lower Hybrid Heating and Current Drive in ITER: Operation Scenarios and Outline System Design,* Association Euratom-CEA, DRFC/CAD, EUR-CEA-FC-1529, (1994).
21. K. Kupfer, D. Moreal and X. Litaudon: *Statistical Theory of Wave Propagation and Multipass Absorption for Current Drive in Tokamakcs*, Association Euratom-CEA, Report EUR-CAE-FC-1496, DRFC/CAD, July, (1993).